DOI: 10.1002/ejic.200601220

Metal Ion Complementarity: Effect of Ring-Size Variation on the Conformation and Stability of Lead(II) and Cadmium(II) Complexes with Pendant-Armed Crowns

Martín Regueiro-Figueroa,[a] David Esteban-Gómez,[a] Carlos Platas-Iglesias,[a] Andrés de Blas,*[a] and Teresa Rodríguez-Blas*[a]

Keywords: Lead / Cadmium / Macrocycles / N,O ligands / Density functional calculations

The binding tendencies of the pendant-armed crown ethers L^1–L^3 [L^1 = *N*,*N*′-bis(benzimidazol-2-ylmethyl)-1,7-diaza-12-crown-4, L^2 = *N*,*N*′-bis(benzimidazol-2-ylmethyl)-1,10-diaza-15-crown-5) and L^3 = *N*,*N*′-bis(benzimidazol-2-ylmethyl)-4,13-diaza-18-crown-6] towards Pb^{II} and Cd^{II} have been investigated. The X-ray crystal structure of $[Cd(L^3)](ClO_4)_2$·EtOH shows that, in the solid state, the Cd^{II} ion is eight-coordinate and fits quite well into the crown hole, favouring an *anti* arrangement of the organic receptor. NMR measurements recorded in acetonitrile solution indicate that increasing the crown size induces a conformational change in the series of Cd^{II} complexes. The conformation goes from a *syn* arrangement for L^1 to an *anti* arrangement for L^3, passing through a *syn* ⇆ *anti* equilibrium in the complex derived from L^2. On the contrary, no conformational change was observed for the corresponding Pb^{II} complexes, which have a *syn* conformation in all cases. These results have been confirmed by means of density functional theory (DFT) calculations performed by using the B3LYP model. The binding constants obtained from UV/Vis titration experiments in DMSO solution demonstrate that a decrease in the crown size provokes a 10^2-fold enhancement of the stability for this series of Cd^{II} complexes, whereas for Pb^{II} a gradual decrease of the binding constants is observed. Receptor L^1 shows a certain degree of selectivity for Cd^{II} over Pb^{II}, with a selectivity factor $> 10^2$.

Introduction

Rational ligand design for selective complexation of metal ions is a field of great interest for chemists. Indeed, selective complexation of metal ions is a condition required for practical applications in many research areas such as the design of ligands as therapeutic reagents for the treatment of metal intoxication, design of antibiotics that owe their antibiotic action to specific metal complexation, design of complexes for imaging agents in the body or design of functional groups for chelating ion-exchange materials, selective metal extractants and metal ion sequestering agents, among others. Some interesting papers and reviews have been written on this subject.[1] Ligand design essentially consists of selecting appropriate donor atoms for the target metal ion and connecting them in an architecture that satisfies the geometric and electronic requirements of the metal ion. Two important concepts must be taken into account for ligand design: preorganization[2] and complementarity.[3] The former may be considered as an entropic effect[4] related to the different conformational states that the ligand can adopt in the free and bound form. Complementarity corresponds to the degree of structural correspondence between the binding sites offered by the ligand structure and the binding sites required by the metal ion. One of the criteria for optimal complementarity is that the metal ion should be able to contact all the donor atoms of the ligand at an optimal metal–donor distance, and therefore the concept of size-match (matching the size of the ligand cavity to the size of the metal ion) must be taken into account in ligand design. Commonly, this has been used as the key concept for the design of complementary ligand architecture; however, many examples have pointed out that when size-match is the sole criterion for the design, the results are often undesired.[1e,5] From the examples given in the literature, it follows that although size-match is a necessary condition for complementarity, it is not sufficient, and that there are other structural factors that must be considered in assessing the degree of metal ion complementarity, in particular the spatial distribution of donor atoms around the metal ion and the orientation of the donor groups.[1e] The application of the complementarity concept is not only restricted to the interaction between a ligand and a given metal ion, but it can also be generalized to any kind of host–guest interaction (i.e. supramolecular assemblies).[6]

[a] Dpto. Química Fundamental, Facultade de Ciencias, Campus da Zapateira s/n, Universidade da Coruña,
15071 A Coruña, Spain
Fax: +34-167065
E-mail: mayter@udc.es
Supporting information for this article is available on the WWW under http://www.eurjic.org or from the author.

In this paper, we report the binding tendencies of the pendant-armed crown ethers L^1–L^3 [L^1 = *N*,*N*′-bis(benzimidazol-2-ylmethyl)-1,7-diaza-12-crown-4, L^2 = *N*,*N*′-bis(benzimidazol-2-ylmethyl)-1,10-diaza-15-crown-5) and L^3 = *N*,*N*′-bis(benzimidazol-2-ylmethyl)-4,13-diaza-18-crown-6; see Scheme 1] towards Pb^{II} and Cd^{II}. The cyclic framework of crown ethers affords an interesting platform for the complexation of metal ions, and they have been commonly used for studying metal ion complementarity. On the other hand, Pb^{II} and Cd^{II} have been selected by taking into account their ionic radius and particular coordination properties. Pb^{II} exhibits the "inert pair effect" and has variable coordination numbers and geometries.[7] The so-called "inert pair effect" refers to the resistance of the pair of outer electrons on Pb^{II} to removal or to participation in covalent bond formation, and it has been explained as a relativistic effect causing the 6s orbital to contract, thereby increasing the energy required to remove or interact with the 6s lone pair of electrons. Likewise, Cd^{II} is capable of considerable plasticity in the lengths of its bonds, and recently Hancock et al.[5] have proved that this metal ion shows an unusual ability to complex almost equally strongly with 12-crown-4, 15-crown-5 and 18-crown-6, in spite of the very different metal ion size requirements of these crown ethers. These authors attribute this behaviour to relativistic effects.

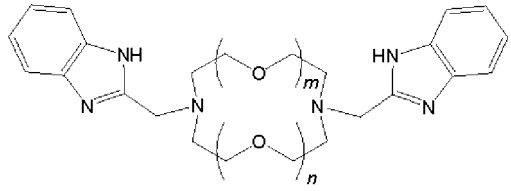

L^1: *m* = 1, *n* = 1
L^2: *m* = 1, *n* = 2
L^3: *m* = 2, *n* = 2

Scheme 1.

Results and Discussion

Synthesis and Characterization of Complexes

The reaction of receptors L^1, L^2 or L^3 (Scheme 1) with Cd^{II} or Pb^{II} perchlorates in absolute ethanol or acetonitrile led to compounds of formula $[Cd(L^1)](ClO_4)_2 \cdot EtOH$ (**1**), $[Pb(L^1)](ClO_4)_2 \cdot 2H_2O$ (**2**), $[Cd(L^2)](ClO_4)_2 \cdot CH_3CN \cdot EtOH$ (**3**), $[Pb(L^2)](ClO_4)_2$ (**4**), $[Cd(L^3)](ClO_4)_2 \cdot EtOH$ (**5**) and $[Pb(L^3)](ClO_4)_2 \cdot EtOH$ (**6**) in good yields (66–76%). The IR spectra (KBr disks) show bands at ca. 1540 and 1120 cm^{-1} due to the ν(C=C) and ν(C–O) stretching frequencies of the benzimidazole and ether groups, respectively. These bands are shifted by 10–15 cm^{-1} to higher wavenumbers with respect to their position in the spectra of the free receptors. The spectra also show absorption bands at ca. 1090 and 625 cm^{-1} attributable to the asymmetric ν_{as}(Cl–O) stretching and δ_{as}(O–Cl–O) bending modes of the perchlorate groups. These bands appear without splitting, as befit uncoordinated anions. The FAB mass spectra of each complex shows intense peaks corresponding to the fragments $[M(L^n)(ClO_4)]^+$ and $[M(L^n–H)]^+$ (L^n = L^1, L^2 or L^3), which confirms the formation of the complexes. Conductivity measurements were carried out in ca. 10^{-3} M acetonitrile solutions at 20 °C. The molar conductivity values revealed that all complexes behave as 2:1 electrolytes in this solvent.[8]

X-ray Crystal Structures

The structure of the uncoordinated receptor L^1 was determined by X-ray diffraction analysis. The receptor crystallizes in the $P2_1/n$ monoclinic space group. The arms of the lariat ether are arranged on the same side of the crown moiety, resulting in a *syn* conformation (Figure 1), with the lone pairs of both pivotal nitrogen atoms directed into the receptor cavity in an *endo-endo* arrangement. The conformation of the receptor is conditioned by two strong intramolecular hydrogen-bonding interactions between the NH groups of the benzimidazole subunits and the oxygen atoms of the crown moiety [N2···O1 2.936(3) Å, N2···H2 0.88(2) Å, O1···H2 2.07(3) Å, N2–H2–O1 166(2)°; N6···O2 2.911(2) Å, N6···H6 0.91(2) Å, O2···H6 2.02(2) Å, N6–H6–O2 = 166(2)°]. The *syn* conformation brings the two benzimidazole units close together, so that intramolecular π–π interactions are possible.[9–11] The distance between the centres of the two rings is 3.681 Å, while the C5–C19 distance amounts to 3.371(3) Å, and the angle between the least-squares planes of the two benzimidazole units is 13.77(7)°.

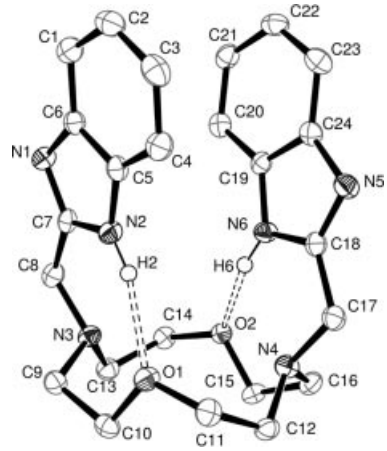

Figure 1. X-ray crystal structure of receptor L^1 with atom labelling; hydrogen atoms are omitted for simplicity; the ORTEP plot is drawn at the 50% probability level.

The solid-state structure of compound **5** was also determined by single-crystal X-ray diffraction analysis. Crystals contain the cation $[Cd(L^3)]^{2+}$, two perchlorate anions and one ethanol molecule. The compound crystallizes in the centrosymmetric $P2_1/c$ monoclinic space group. One of the perchlorate anions and the ethanol molecule are quite disordered: the site occupancy factor is 0.776(5) for the perchlorate group [Cl1A, O10A, O11A, O12A and O13A], and 0.641(9) for the ethanol molecule [O100, C100 and C101].

Table 1 summarizes selected bond lengths of the metal coordination environment, while Figure 2 displays a view of the structure of the cation. The complex cation $[Cd(L^3)]^{2+}$ contains a CdN_4O_4 core in which the eight heteroatoms of L^3 are coordinated to the metal ion. The organic receptor L^3 adopts an *anti* arrangement in which both benzimidazole pendant arms are disposed on opposite sides of the crown moiety. The Cd^{II} ion is asymmetrically placed inside the macrocyclic ring, being closer to the donor atoms O2 and O3 [Cd1–O2: 2.585(2) Å; Cd1–O3: 2.526(2) Å] than to O1 and O4 [Cd1–O1: 2.594(2) Å; Cd1–O4: 2.604(2) Å]. The distances between Cd^{II} and the two pivotal nitrogen atoms differ by ca. 0.1 Å [Cd1–N3: 2.516(3) Å and Cd1–N4: 2.627(3) Å], whereas the distances between Cd^{II} and nitrogen atoms of the benzimidazole groups are similar and fall within the range reported for Cd–N distances in complexes with ligands containing benzimidazole groups.[12,13] On the other hand, the distances between the metal ion and nitrogen pivotal atoms and oxygen atoms of the crown moiety are ca. 0.2 Å longer than those observed in a cadmium(II) cryptate derived from 1,10-diaza-15-crown-5 containing a pyridinyl Schiff base spacer, where the metal ion is seven-coordinate.[14] The Cd–O bond lengths are also ca. 0.2 Å longer than those observed for Cd^{II} complexes of 12-crown-4[15] and 15-crown-5,[16] but similar to those observed for different Cd^{II} complexes of 18-crown-6.[16] These data reflect the ability of Cd^{II} to change Cd–O bond lengths to meet the requirements of crown ethers of different size, which has been attributed to relativistic effects.[5] Relativistic effects lower the energy of the valence shell s orbital next in energy to a filled d orbital in heavy d^{10} metal ions, which leads to a tendency to sp hybridization and the formation of more covalent M–L bonds.[17] In the case of compound **5**, the presence of two axial nitrogen donor atoms of the benzimidazole groups [N1 and N5] causes a distortion toward linear coordination geometry with long equatorial Cd–O bonds.

Table 1. Selected bond lengths [Å] and angles [°] of the metal coordination environment in $[Cd(L^3)]^{2+}$.

Cd1–N1	2.287(2)	Cd1–O3	2.526(2)
Cd1–N5	2.245(2)	Cd1–O4	2.604(2)
Cd1–O1	2.594(2)	Cd1–N3	2.516(3)
Cd1–O2	2.585(2)	Cd1–N4	2.627(3)
N5–Cd1–N1	158.78(8)	O2–Cd1–O1	64.18(7)
N5–Cd1–N3	111.85(9)	N5–Cd1–O4	80.91(7)
N1–Cd1–N3	74.01(8)	N1–Cd1–O4	119.22(7)
N5–Cd1–O3	121.09(8)	N3–Cd1–O4	66.64(8)
N1–Cd1–O3	76.91(7)	O3–Cd1–O4	64.10(7)
N3–Cd1–O3	96.35(8)	O2–Cd1–O4	157.23(7)
N5–Cd1–O2	78.04(8)	O1–Cd1–O4	122.98(7)
N1–Cd1–O2	82.85(8)	N5–Cd1–N4	71.32(9)
N3–Cd1–O2	129.99(8)	N1–Cd1–N4	109.83(8)
O3–Cd1–O2	120.95(7)	N3–Cd1–N4	161.82(8)
N5–Cd1–O1	86.05(8)	O3–Cd1–N4	68.16(7)
N1–Cd1–O1	77.30(7)	O2–Cd1–N4	68.00(7)
N3–Cd1–O1	67.73(8)	O1–Cd1–N4	130.26(7)
O3–Cd1–O1	152.65(7)	O4–Cd1–N4	97.07(7)

The coordination polyhedron around the Cd^{II} ion can be described as a distorted square antiprism composed of two

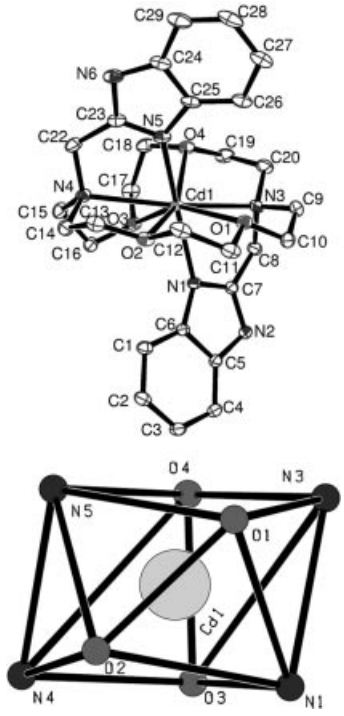

Figure 2. Top: X-ray crystal structure of the cation $[Cd(L^3)]^{2+}$ in compound **5** with atom labelling; hydrogen atoms are omitted for simplicity; the ORTEP plot is drawn at the 30% probability level. Bottom: Coordination polyhedron around Cd^{II} in compound **5**.

parallel pseudoplanes (see Figure 2): O1, O4, N3 and N5 define the upper pseudoplane (mean deviation from planarity 0.0889 Å), while O2, O3, N4 and N1 define the lower pseudoplane (mean deviation from planarity 0.0982 Å). The angle between the two least-squares planes is 9.14°. The mean twist angle, ω,[18] between these nearly parallel squares is 26.0°, showing a deformation of the coordination polyhedron from a square antiprism (ideal value 45°) toward a square prism (ideal value 0°) by ca. 19°.

Solution Structure

The behaviour of compounds **1** to **6** in [D_3]acetonitrile solution was investigated by ^1H and ^{13}C NMR spectroscopy. The spectra were assigned on the basis of two-dimensional COSY, HSQC and HMBC experiments. Significant changes in the chemical shifts, the structures of the signals and even the number of signals are observed in the ^1H NMR spectra upon coordination of the ligands to the metal ions (Tables S1–S3, Supporting Information). The most complicated region of the spectra is the part where the ethylene and methylene proton signals are observed. The coordination to the metal ion increases the rigidity of the ligand, limiting conformational exchange processes, so that the geminal CH_2 protons are no longer equivalent. Since assignments to specific axial/equatorial CH_2 protons were not possible on the basis of the 2D NMR spectra, they were carried out by using the stereochemical dependence of their shifts on the polarization of the C–H bonds derived from

the coordination of the metal ion.[19] This polarization results in a deshielding of the equatorial protons, which point away from the metal ion. The aromatic region appears to be usually more clearly resolved for metal ion complexes than for free ligands. This is due to the presence in the latter of exchange processes involving the NH and N positions of the benzimidazole groups that are prevented by coordination to the metal ion.

The ^{13}C NMR spectra of **1** and **2** display ten resonances for the 24 proton nuclei present in the ligand backbone, in agreement with an effective C_{2v} symmetry for both complexes in solution. Upon coordination to the metal ion, the signals corresponding to the ethylene and methylene protons shift downfield (Figure 3), confirming the coordination of the ligand in the complexes. The ethylene protons at the five-membered chelate rings formed by the coordination of the ligand to the metal ion give an AA′XX′ spectrum, where the equatorial protons are more deshielded by the electric field effect of the cation (Figure 3). The methylene proton signals of the pendant arms in the ^1H NMR spectra of **1** and **2** show satellites attributable to proton coupling to the naturally abundant ^{113}Cd (I = 1/2) and ^{207}Pb (I = 1/2), respectively, reflecting kinetic inertness in the complexes as well as a degree of covalence in the interaction with the nearby donor atom. So, the signals at δ = 4.28 ppm for **1** and δ = 4.51 ppm for **2** appear as a singlet flanked by the satellites, with a $^3J(H_8–^{113}Cd)$ of 9.96 Hz and $^3J(H_8–^{207}Pb)$ of 10.10 Hz. A $^3J(H–^{113}Cd)$ of 8.00 Hz has been reported for the methylene protons of a Cd^{II} complex with a multidentate nitrogen receptor, for which a Cd–N bond length of 2.53 Å was found in the solid state,[20] while $^3J(H–^{207}Pb)$ values of 14.30 and 17.00 Hz have been observed for $[Pb(EDTA–N_4)]^{2+}$, where the Pb–N bond length in the solid state was found to be 2.61 Å.[21]

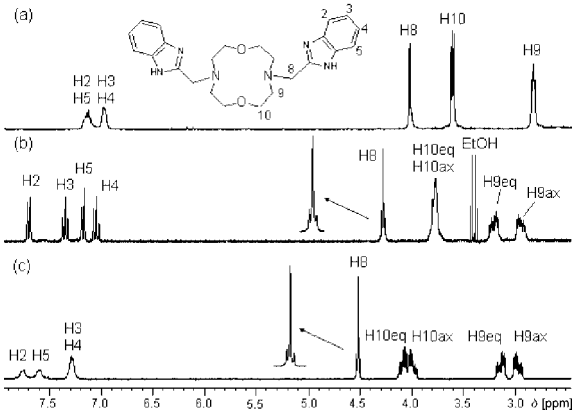

Figure 3. ^1H NMR spectra of (a) L^1, (b) compound **1** and (c) compound **2** as recorded in [D_3]acetonitrile solution at 298 K.

The ^1H NMR spectrum of **3** shows two different resonances with different intensities for the NH groups of the benzimidazole subunits, which suggests the presence of two different isomers of **3** in acetonitrile solution. The spectrum recorded at 298 K displays broad resonances for the signals of the aromatic protons, but the signals become better resolved upon decreasing the temperature below 233 K. A detailed analysis of the ^1H and ^{13}C NMR spectra at this temperature clearly confirms the presence of two complex species in solution that are in equilibrium. The signals corresponding to both species were fully assigned with the aid of two-dimensional COSY, HSQC and HMBC spectra (Table S2, Supporting Information). The ^1H NMR spectrum of **3** recorded at 233 K is shown in Figure 4a. The spectrum of the major species shows 26 resonances in the ^{13}C NMR spectrum, indicating C_1 symmetry in solution, while the minor species shows 13 resonances, which indicates an effective C_2 symmetry of the complex where the benzimidazole pendant arms are equivalent. In a previous work, we reported a similar situation for lanthanide complexes with lariat ethers derived from 1,10-diaza-15-crown-5 containing salicylaldimine groups, which show a *syn* conformation with a C_1 symmetry.[11] A striking feature of the ^1H NMR spectrum of the species with C_1 symmetry is the unusually large low-frequency shift found for the signal of the H5′ protons (δ =6.18 ppm, Figure 4a). Similar shielding effects have been observed in lanthanide complexes with lariat ethers having a *syn* conformation, which have been explained by the observation that these protons are directed toward the aromatic ring current of the neighbouring pendant arm.[22] On this basis, we assign the major species of $[Cd(L^2)]^{2+}$ in solution, which shows C_1 symmetry, to a complex with a *syn* arrangement of the pendant arms, while the minor species (with an effective C_2 symmetry in solution) is assigned to an *anti* isomer. An equilibrium in solution between the *syn* and *anti* conformations has been previously reported for Ba^{II} complexes with pendant-armed crowns derived from 4,13-diaza-18-crown-6.[23] The smaller Cd^{II} ion fits quite well inside the crown moiety hole of L^2, which makes possible an equilibrium between *syn* and *anti* isomers in acetonitrile solution. To confirm this we have performed DFT calculations at the B3LYP level on the $[Cd(L^2)]^{2+}$ system. Our calculations provide two minimum-energy conformations for $[Cd(L^2)]^{2+}$, which correspond to the *syn* and *anti* isomers (Figure 5). The calculated geometry for the *syn*

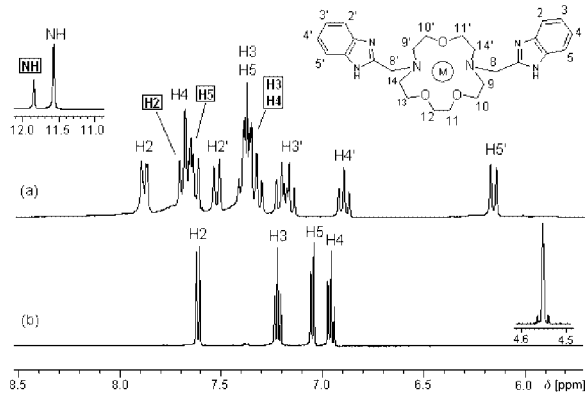

Figure 4. (a) Partial ^1H NMR spectrum of compound **3** recorded in [D_3]acetonitrile at 233 K. The labels within rectangles correspond to the signals of the *anti* isomer (effective C_2 symmetry), while the remaining ones denote signals of the *syn* one (C_1 symmetry). (b) Partial ^1H NMR spectrum of compound **4** recorded in [D_3]acetonitrile at 298 K.

isomer shows the H5′ proton placed above the plane of the benzimidazole group of the neighbour pendant arm, in agreement with the high-field shift observed for this proton in the NMR spectrum.

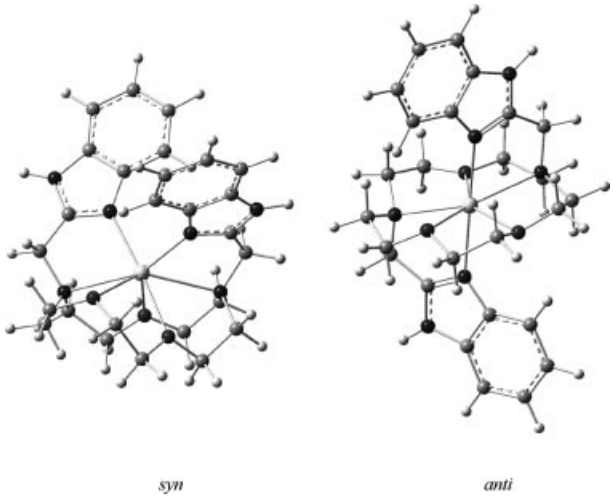

Figure 5. Structures of the two isomers of $[Cd(L^2)]^{+2}$ obtained from DFT calculations at the B3LYP level.

The equilibrium between the *syn* and *anti* isomers of $[Cd(L^2)]^{2+}$ is shown in Equation (1).

$$[Cd(L^2)]^{2+}_{syn} \leftrightarrows [Cd(L^2)]^{2+}_{anti} \quad (1)$$

The equilibrium constant defined by Equation (1), K_{eq}, was determined at several temperatures between 233 to 294 K from the relative integrations of the ^{1}H NMR signals due to the NH protons of the benzimidazole groups. The ratio between the intensity of the peaks corresponding to the *syn* and *anti* species was found to be constant within experimental error in the range of temperatures studied. This indicates that $\Delta S^0 \approx 0$ for the interconversion process described by Equation (1), in agreement with an intramolecular rearrangement. From the ^{1}H NMR in acetonitrile solution, we obtain $K_{eq} = 0.33 \pm 0.02$, pointing out that the *syn* isomer predominates in acetonitrile solution at any temperature.

The ^{1}H NMR spectrum of the Pb^{II} derivative **4** (Figure 4b) is clearly more simple than that of the corresponding Cd^{II} analogue. In this case, a single species with an effective C_s symmetry in solution is observed. This is confirmed by the ^{13}C NMR spectrum, which shows 13 signals for the 26 nuclei of the ligand backbone (Table S2, Supporting information). DFT calculations predict a *syn* conformation for the receptor in the $[Pb(L^2)]^{2+}$ system, where the metal ion is placed over the crown moiety interacting with all the donor atoms present in the receptor (Figure S1, Supporting Information). An identical situation has been observed in complexes with lariat ethers derived from 1,10-diaza-15-crown-5.[14] It may be surprising to observe an effective C_s symmetry for $[Pb(L^2)]^{2+}$ while the analogous $[Cd(L^2)]^{2+}$ *syn* isomer displays a C_1 symmetry in solution. This can be explained if one considers the smaller size of Cd^{II} compared to Pb^{II}, which allows the two benzimidazole pendants to adopt a face-to-face conformation (Figure 6). In $[Pb(L^2)]^{2+}$ the two pendant arms adopt a more open conformation (see Figure 5 and Figure S1, Supporting Information), which allows an easy interconversion between the two optical isomers (Δ and Λ) characteristic of the *syn* conformation.[24] When this interconversion is fast enough on the ^{1}H NMR time scale, an effective C_s symmetry in solution is observed (Figure 6).

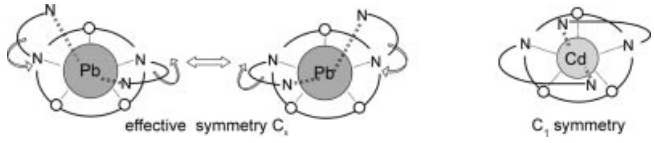

Figure 6. Schematic representation of the different *syn* conformations adopted by lariat ethers derived from 1,10-diaza-15-crown-5 depending on the size of the metal ion.

As observed for the complex of L^1, the ^{1}H NMR spectrum of $[Pb(L^2)]^{2+}$ shows the singlet due to the H8 protons at $\delta = 4.52$ ppm flanked by satellites with a $^3J(H_8–^{207}Pb)$ of 20.40 Hz (Figure 4b), reflecting a strong interaction between Pb^{II} and the coordinated nitrogen pivot atoms of the receptor. This value is much higher than that observed for the analogous complex derived from L^1 (10.10 Hz, vide supra), suggesting that a greater crown size favours a better fit between the Pb^{II} ions and the macrocyclic cavity.

The ^{13}C NMR spectrum of **5** displays eleven resonances for the 28 carbon nuclei present in the ligand backbone, in agreement with an effective C_{2h} symmetry in solution. This is consistent with an *anti* arrangement of the pendant arms in the complex, as observed in the solid-state structure of this compound described above. In the ^{1}H NMR spectra (Figure 7), the signals corresponding to the ethylene protons are again complicated because of the coordination to the metal ion. The signal of the methylene protons of the pendant arms appears as a singlet flanked by the satellites attributable to proton coupling to the naturally abundant ^{113}Cd ($I = 1/2$) at $\delta = 4.25$ ppm with a $^3J(H_8–^{113}Cd)$ of 7.41 Hz. If we compare this value with that found for **1** (9.96 Hz) we can conclude that, for Cd^{II}, increasing the crown size weakens the interaction between the metal ion and the coordinated pivotal nitrogen atoms.

Unlike the Cd^{II} analogue, the ^{1}H NMR and the ^{13}C NMR spectra of the lead(II) complex **6**, (Figure 7b) registered at 233 K are in agreement with an effective C_2 symmetry of the complex in solution. The ^{1}H-^{1}H COSY spectrum clearly shows a coupling between protons H11 and H12 (see the labelling scheme in Figure 7), which indicates that the C_2 axis of the complex is perpendicular to the pseudoplane formed by the donor atoms of the crown moiety. This result indicates a *syn* arrangement of the receptor in the complex.[24] The H8 protons appear as an AB spin system ($^2J_{8a,8b} = 18.40$ Hz) in the spectrum of **6**, while a singlet is observed for the H8 protons in the Cd^{II} analogue **5**. These results are in agreement with a *syn* conformation of the Pb^{II} complex with the pendant arms adopting a face-to-face conformation, as observed for $[Cd(L^2)]^{2+}$.

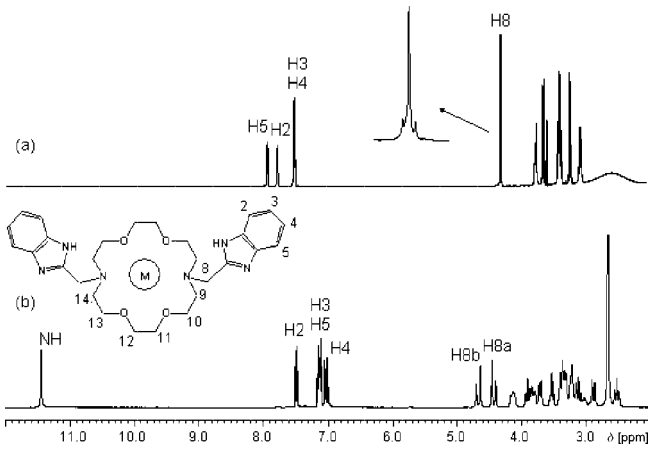

Figure 7. ^{1}H NMR spectra of compounds (a) **5** and (b) **6** recorded in [D_3]acetonitrile at 298 K.

In order to obtain structural information on this complex in solution we performed geometry optimizations of the $[Pb(L^3)]^{2+}$ system. Our DFT calculations predict two minimum-energy conformations corresponding to a *syn* and an *anti* conformation (Figure S2, Supporting Information). From the conformational energies of the *syn* and *anti* isomers of $[Pb(L^3)]^{2+}$ we have calculated an in vacuo relative free energy, $\Delta G°_{298K} = G°_{anti} - G°_{syn}$, of 3.54 kcal mol^{-1}. Likewise, from the results obtained in acetonitrile solution (COSMORS model) we have obtained a relative free energy, $\Delta G^{sol} = G^{sol}_{anti} - G^{sol}_{syn}$, of 4.79 kcal mol^{-1}. Thus, our quantum mechanical calculations predict that the *syn* isomer is the most stable one both in vacuo and in solution. These results confirm that the complex adopts a *syn* conformation in solution. This situation contrasts that observed for a related lead(II) complex derived from the same crown moiety and containing aniline pendants, for which an *anti* arrangement of the receptor was found.[25] In that complex, the aniline pendants form six-membered chelate rings upon coordination to the metal ion, which probably favour an *anti* arrangement of the macrocyclic receptor in the complex.

Stability of the Complexes in Solution

The binding of Cd^{II} and Pb^{II} by the three receptors was investigated by means of spectrophotometric titrations in DMSO solution. The electronic spectra of the free ligands show two typical absorption bands in the near UV attributable to the benzimidazole groups, which can be assigned as $\pi^* \leftarrow \pi$ singlet–singlet transitions[26] ($^1L_a \leftarrow S_0$ and $^1L_b \leftarrow S_0$, where the two excited states are labelled by ^1L_a and ^1L_b following the suggestion of Platt).[27] Addition of the metal ion salt causes appreciable modification of the spectral patterns. In particular, metal ion addition induces blue shifts of the bands centred at 277 and 284 nm as their intensity increases. These results indicate the coordination of the benzimidazole groups to the metal ion in this solvent. In the course of the titration of Cd^{II} with L^3, the development of a weak band centred at ca. 330 nm is also observed. The family of UV/Vis spectra recorded over the course of the titrations of L^1 and L^3 with Cd^{II} are shown in Figure 8. Nonlinear least-squares analysis of the titration profiles (absorbance against the number of equivalents of Cd^{II}, see insets of Figure 8) clearly indicates the formation of 1:1 complexes in every case; the association constants are summarized in Table 2. In all cases, the three ligands form stable complexes with both Cd^{II} and Pb^{II} ($\log K > 5$, Table 2). For $[Cd(L^1)]^{2+}$ the steep curvature of the profile at the addition of 1 equiv. prevents a safe determination of the binding constant, and a lower threshold value of $\log K > 7.5$ can be estimated (Figure 8).

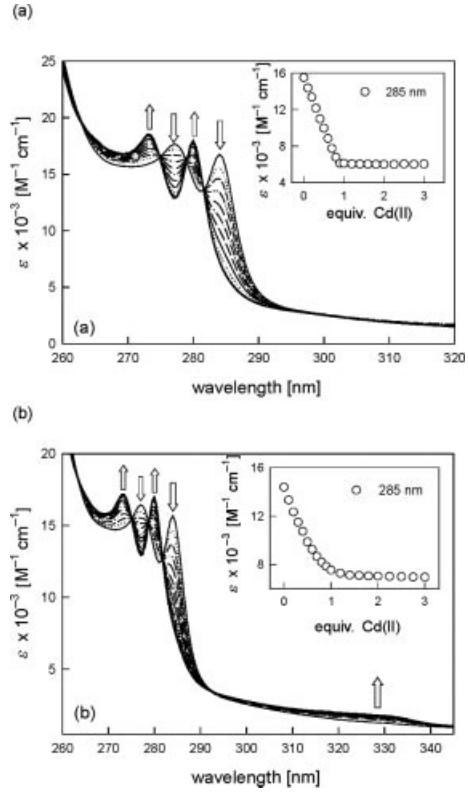

Figure 8. Spectra recorded over the course of the titration of a 10^{-4} M solution of (a) L^1 and (b) L^3 with a standard solution of cadmium(II) perchlorate. Insets: titration profiles at selected wavelengths.

Table 2. Binding constants of the Cd^{II} and Pb^{II} complexes with L^1, L^2 and L^3 obtained from spectrophotometric titrations in DMSO solutions at 25 °C. Log K refers to $L^n + M^{2+} \leftrightarrows [ML^n]^{2+}$.[a]

Ligand	Ring size	$\log K_{Cd^{II}}$	$\log K_{Pb^{II}}$
L^1	12	>7.5[b]	5.65(5)
L^2	15	6.23(3)	6.15(5)
L^3	18	5.41(1)	6.63(9)

[a] The errors given correspond to one statistical deviation; the experimental errors are estimated to be ±0.2 log K units. [b] The complex is too stable to allow a safe determination of the binding constant.

The log K values obtained show different trends in the binding of Cd^{II} and Pb^{II} on changing the macrocyclic ring size. For Cd^{II}, a gradual decrease of the binding constants is observed as the macrocyclic ring size increases, while the Pb^{II} complexes show the opposite behaviour. As a result,

receptor L^1 shows a certain degree of selectivity for Cd^{II} over Pb^{II}, with a selectivity factor $> 10^2$. It is interesting to note that the stability of Cd^{II} complexes with crown ethers such as 18-crown-6, 15-crown-5 or 12-crown-4 increases as the macrocyclic cavity is enlarged.[5] Thus, the introduction of pendant arms into the framework of these crown ethers appears to reverse this trend, revealing the complementarity of L^1 and Cd^{II}.

The binding affinity trend of the above ligand series toward Pb^{II} is probably the result of a better size-match of the ligand for this metal ion as the size of the crown moiety increases. Moreover, Pb^{II} usually prefers higher coordination numbers than Cd^{II}, and therefore one expects an increasing stability of the Pb^{II} complexes with this series of ligands as the number of oxygen atoms of the crown moiety increases. The introduction of an oxygen atom into the crown moiety increases the stability of the corresponding Pb^{II} complex by ca. 0.5 $\log K$ units. The Pb^{II} complex of L^3 is more stable than the Cd^{II} analogue by ca. 1 $\log K$ units. A similar difference in the $\log K$ values has been previously reported for Pb^{II} and Cd^{II} complexes of a bibracchial lariat ether derived from diaza-18-crown-6 containing 5-chloro-8-methoxyquinoline pendants ($\log K_{Pb}$ = 7.0 and $\log K_{Cd}$ = 6.1 in MeOH).[28] The binding tendencies discussed above for the Pb^{II} and Cd^{II} complexes described in this work parallel the $^3J(H_8–^{113}Cd)$ and $^3J(H_8–^{207}Pb)$ coupling constants observed in the ^1H NMR spectra recorded in acetonitrile solution (vide supra), which are related to the strength of the interaction between the cation and the pivotal nitrogen atoms of the ligand.

Conclusions

The pendant-armed macrocycles L^1, L^2 and L^3 (L^1 = *N*,*N*′-bis(benzimidazol-2-ylmethyl)-1,7-diaza-12-crown-4, L^2 = *N*,*N*′-bis(benzimidazol-2-ylmethyl)-1,10-diaza-15-crown-5) and L^3 = *N*,*N*′-bis(benzimidazol-2-ylmethyl)-4,13-diaza-18-crown-6) form mononuclear complexes with both Cd^{II} and Pb^{II}. NMR measurements recorded in acetonitrile solution indicate that increasing the crown size induces a conformational change in the series of cadmium(II) complexes that goes from a *syn* arrangement for L^1 to an *anti* arrangement for L^3, passing through a *syn* ⇆ *anti* equilibrium in the complex derived from L^2. The X-ray structure of the $[Cd(L^3)]^{2+}$ complex confirms the *anti* arrangement observed in acetonitrile solution. On the contrary, no conformational change was observed for the corresponding lead(II) complexes, which show a *syn* conformation in all cases. DFT calculations (B3LYP model) support the results of the conformational analyses performed on the basis of the NMR spectroscopic data. The binding constants obtained from UV/Vis titration experiments in DMSO solution indicate that a diminution of the crown moiety size provokes a $> 10^2$-fold enhancement of the stability for this series of Cd^{II} complexes, whereas for Pb^{II} a smooth decrease of the binding constants is observed. Receptor L^1 shows a certain degree of selectivity for Cd^{II} over Pb^{II}, with a selectivity factor $> 10^2$.

Experimental Section

General Considerations: All chemicals were purchased from commercial sources and used without further purification. Solvents were of reagent grade and were purified by the usual methods. *N*,*N*′-Bis(benzimidazol-2-ylmethyl)-4,13-diaza-18-crown-6 (L^3) was prepared according to the literature method.[29] ***Caution!*** Although we have experienced no difficulties with perchlorate salts, these should be regarded as potentially explosive and handled with care.[30]

Elemental analyses were carried out with a Carlo Erba 1108 elemental analyzer. FAB mass spectra were recorded by using a FISONS QUATRO mass spectrometer with Cs ion gun in a 3-nitrobenzyl alcohol matrix. ^1H and ^{13}C NMR spectra were recorded with a Bruker AMX300 or a Bruker WM-500 spectrometer. IR spectra were recorded, as KBr discs, by using a Bruker Vector 22 spectrometer. Conductivity measurements were carried out at 20 °C with a Crison Micro CM 2201 conductimeter by using ca.10^{-3}-M solutions of the complexes in acetonitrile. UV/Vis spectra were recorded with a Perkin–Elmer Lambda 900 spectrophotometer, in quartz cells (path length: 1 cm). The cell holder was thermostatted at 25.0 °C with circulating water. Spectrophotometric titrations were performed at 25 °C on 10^{-4}-M solutions of the ligand in DMSO (polarographic grade). Typically, aliquots of a fresh standard solution of the envisaged perchlorate salt (Pb or Cd, 10^{-2} M) were added and the UV/Vis spectra of the samples were recorded. All spectrophotometric titration curves were fitted with the HYPERQUAD program.[31]

Preparation of the Ligands

***N*,*N*′-Bis(benzimidazol-2-ylmethyl)-1,7-diaza-12-crown-4 (L^1):** 1,7-Diaza-12-crown-4 (1.0 g, 5.7 mmol), *N*,*N*-diisopropylethylamine (4.0 mL, 23.1 mmol) and 2-(chloromethyl)benzimidazole (2.1 g, 12.7 mmol) in acetonitrile (200 mL) were heated under reflux for 12 h and cooled to room temperature. The reaction mixture was concentrated in a rotary evaporator and after being kept at –4 °C for 24 h, a brown precipitate was filtered off and the filtrate was concentrated under vacuum. The resulting yellow oily residue was extracted with CH_2Cl_2/water, and the organic phase was dried with anhydrous $MgSO_4$ and concentrated in vacuo. Addition of cold diethyl ether to the oily residue led to the deposition of a light yellow precipitate, which was purified by column chromatography on Al_2O_3 with a CH_2Cl_2/MeOH 2% mixture as eluent to give a brown solid (1.7229 g, 65%). $C_{24}H_{30}N_6O_2{\cdot}0.5CH_3CN{\cdot}0.5H_2O$ (475.08): calcd. C 64.70, H 7.06, N 19.62; found C 65.32, H 7.83, N 19.36. M.p. 190 °C. ^1H NMR (300 MHz, $CDCl_3$, 25 °C): δ = 2.90 (t, $^3J_{H,H}$ = 4.6 Hz, 8 H), 3.66 (t, $^3J_{H,H}$ = 4.6 Hz, 8 H), 4.10 (s, 4 H), 7.14–7.08 (m, 4 H), 7.66 (br., 4 H), 11.56 (br., 2 H) ppm. ^{13}C NMR (75.5 MHz, $CDCl_3$, 25 °C): δ = 53.8, 55.4, 69.0, 122.6, 153.8 ppm. MS (FAB): *m*/*z* (%BPI) = 435 (100) $[C_{24}H_{30}N_6O_2]^+$. IR (KBr): $\tilde{\nu}$ = 1623 [ν(C=N)], 1531 [ν(C=C)], 1443 [δ(N–H)], 1428 [$\delta(C–H)_{ar}$], 1355, 1274 [$\delta(C–H)_{crown}$], 1104 [ν(C–O)], [ν(C–N) and ν(C–C)], 744 [π(C–H) and π(N–H)] cm^{-1}. Single crystals of L^1 suitable for X-ray diffraction were grown by recrystallization from acetonitrile.

***N*,*N*′-Bis(benzimidazol-2-ylmethyl)-1,10-diaza-15-crown-5 (L^2):** 1,10-Diaza-15-crown-5 (1.0 g, 4.7 mmol), *N*,*N*-diisopropylethyl amine (3.2 mL, 18.4 mmol) and 2-(chloromethyl)benzimidazole (1.7 g, 10.1 mmol) in acetonitrile (200 mL) were heated under reflux for 12 h and cooled to room temperature. The reaction mixture was concentrated in a rotary evaporator and after being kept at –4 °C overnight, the precipitate formed was filtered and air-dried to give a brown solid (1.2411 g, 52%). $C_{26}H_{34}N_6O_3{\cdot}0.5CH_3CN{\cdot}H_2O$

(507.81): calcd. C 62.71, H 7.31, N 17.61; found C 63.41, H 7.73, N 17.63. M.p. 228 °C. ^{1}H NMR (300 MHz, $CDCl_3$, 25 °C): δ = 2.84 (t, $^3J_{H,H}$ = 4.7 Hz, 4 H), 2.96 (t, $^3J_{H,H}$ = 4.7 Hz, 4 H), 3.40 (t, $^3J_{H,H}$ = 4.7 Hz, 4 H), 3.58–3.53 (m, 8 H), 4.03 (s, 4 H), 7.22–7.16 (m, 4 H), 7.55 (br., 4 H) ppm. ^{13}C NMR (75.5 MHz, $CDCl_3$, 25 °C): δ = 54.1, 56.8, 57.0, 68.5, 69.7, 121.9, 154.7 ppm. MS (FAB): *m/z* (%BPI) = 479 (100) $[C_{26}H_{34}N_6O_3]^+$. IR (KBr): $\tilde{\nu}$ = 1621 [ν(C=N)], 1520 [ν(C=C)], 1455 [δ(N–H)], 1422 [δ(C–H)$_{ar}$], 1346, 1273 [δ(C–H)$_{crown}$], 1106 [ν(C–O)], [ν(C–N) and ν(C–C)], 752 [π(C–H) and π(N–H)] cm^{-1}.

Preparation of the Lead(II) and Cadmium(II) Complexes

General Procedure: A stoichiometric amount (1:1) of the corresponding metal salt was added to a stirred solution of ligand (0.100 g) in absolute ethanol or acetonitrile (50 mL). The mixture was vigorously stirred and heated for 4 h, and the resulting pale-yellow solution was filtered while hot. Quantities of reactants, isolation procedures and characterization of the compounds are described below for each compound.

[Cd(L^1)](ClO$_4$)$_2$·EtOH (1): Solvent: absolute ethanol. Cd(ClO$_4$)$_2$·3H$_2$O (0.096 g, 0.230 mmol). Slow diffusion of diethyl ether into the former solution at room temperature produced pale-yellow crystals that were collected by filtration and air-dried (0.113 g, 62%). $C_{26}H_{36}CdCl_2N_6O_{11}$ (791.91): calcd. C 39.43, H 4.58, N 10.61; found C 39.88, H 4.58, N 10.90. Λ_M (acetonitrile) = 264 cm^{2}Ω^{-1}mol^{-1} (2:1 electrolyte). MS (FAB): *m/z* (%BPI) = 647 (70) $[Cd(L^1)(ClO_4)]^+$, 547 (100) $[Cd(L^1–H)]^+$. IR (KBr): $\tilde{\nu}$ = 1622 [ν(C=N)], 1542 [ν(C=C)], 1456 [δ(N–H) δ(C–H)$_{ar}$], 1339, 1277 [δ(C–H)$_{crown}$], 1113 [ν(C–O)], 758 [π(C–H)], 1090 [ν$_a$(Cl–O)], 623 [δ$_a$(O–Cl–O)] cm^{-1}.

[Pb(L^1)](ClO$_4$)$_2$·2H$_2$O (2): Solvent: absolute ethanol. Pb(ClO$_4$)$_2$·3H$_2$O (0.106 g, 0.230 mmol). Slow diffusion of diethyl ether into the former solution at room temperature produced pale-yellow crystals that were collected by filtration and air-dried (0.132 g, 66%). $C_{24}H_{34}Cl_2PbN_6O_{12}$ (876.67): calcd. C 32.88, H 3.91, N 9.59; found C 32.80, H 4.13, N 9.54. Λ_M (acetonitrile): 276 cm^{2}Ω^{-1}mol^{-1} (2:1 electrolyte). MS (FAB): *m/z* (%BPI) = 741 (100) $[Pb(L^1)(ClO_4)]^+$, 641 (85) $[Pb(L^1–H)]^+$. IR (KBr): $\tilde{\nu}$ = 1621 [ν(C=N)], 1536 [ν(C=C)], 1481 [δ(N–H)], 1452 [δ(C–H)$_{ar}$], 1340, 1274 [δ-(C–H)$_{crown}$], 1118 [ν(C–O)], 762 [π(C–H)], 1086 [ν$_a$(Cl–O)], 625 [δ$_a$(O–Cl–O)] cm^{-1}.

[Cd(L^2)](ClO$_4$)$_2$·CH$_3$CN·EtOH (3): Solvent: acetonitrile. Cd(ClO$_4$)$_2$·3H$_2$O (0.109 g, 0.259 mmol). The reaction mixture was concentrated in a rotary evaporator and addition of cold diethyl ether to the residue led to the deposition of a brown precipitate that was filtered and air-dried (0.155 g, 72%). $C_{30}H_{43}CdCl_2N_7O_{12}$ (877.02): calcd. C 41.08, H 4.94, N 11.18; found C 41.73, H 4.95, N 11.20. Λ_M (acetonitrile) = 251 cm^{2}Ω^{-1}mol^{-1} (2:1 electrolyte). MS (FAB): *m/z* (%BPI) = 691 (15) $[Cd(L^2)(ClO_4)]^+$, 591 (65) $[Cd(L^2–H)]^+$. IR (KBr): $\tilde{\nu}$ = 1622 [ν(C=N)], 1539 [ν(C=C)], 1452 [δ(N–H) δ(C–H)$_{ar}$], 1333, 1273 [δ(C–H)$_{crown}$], 1117 [ν(C–O)], 752 [π(C–H)], 1088 [ν$_a$(Cl–O)], 626 [δ$_a$(O–Cl–O)] cm^{-1}.

[Pb(L^2)](ClO$_4$)$_2$ (4): Solvent: absolute ethanol. Pb(ClO$_4$)$_2$·3H$_2$O (0.108 g, 0.235 mmol). Slow evaporation of the filtrate produced white crystals that were collected by filtration and air-dried (0.145 g, 70%). $C_{26}H_{34}Cl_2PbN_6O_{11}$ (884.69): calcd. C 35.30, H 3.87, N 9.50; found C 35.16, H 4.10, N 9.52. Λ_M (acetonitrile): 300 cm^{2}Ω^{-1}mol^{-1} (2:1 electrolyte). MS (FAB): *m/z* (%BPI) = 785 (80) $[Pb(L^2)(ClO_4)]^+$, 685 (100) $[Pb(L^2–H)]^+$. IR (KBr): $\tilde{\nu}$ = 1621 [ν(C=N)], 1536 [ν(C=C)], 1452 [δ(N–H) δ(C–H)$_{ar}$], 1337, 1272 [δ(C–H)$_{crown}$], 1121 [ν(C–O)], 752 [π(C–H)], 1090 [ν$_a$(Cl–O)], 621 [δ$_a$(O–Cl–O)] cm^{-1}.

[Cd(L^3)](ClO$_4$)$_2$·EtOH (5): Solvent: absolute ethanol. Cd(ClO$_4$)$_2$·3H$_2$O (0.086 g, 0.191 mmol). Slow evaporation of the filtrate produced pale-brown crystals that were collected by filtration and air-dried (0.107 g, 64%). $C_{30}H_{44}CdCl_2N_6O_{13}$ (880.02): calcd. C 40.94, H 5.04, N 9.55; found C 41.09, H 5.27, N 9.76. Λ_M (acetonitrile): 282 cm^{2}Ω^{-1}mol^{-1} (2:1 electrolyte). MS (FAB): *m/z* (%BPI) = 735 (20) $[Cd(L^3)(ClO_4)]^+$, 635 (100) $[Cd(L^3–H)]^+$. IR (KBr): $\tilde{\nu}$ = 1624 [ν(C=N)], 1540 [ν(C=C)], 1471 [δ(N–H)], 1453 [δ(C–H)$_{ar}$], 1345, 1269 [δ(C–H)$_{crown}$], 752 [π(C–H)], 1090 [ν$_a$(Cl–O)], 625 [δ$_a$(O–Cl–O)] cm^{-1}. Single crystals of formula [Cd(L^3)](ClO$_4$)$_2$·EtOH suitable for X-ray diffraction were grown by slow diffusion of diethyl ether into solutions of the complex in acetonitrile.

[Pb(L^3)](ClO$_4$)$_2$·EtOH (6): Solvent: absolute ethanol. Pb(ClO$_4$)$_2$·3H$_2$O (0.088 g, 0.191 mmol). Slow evaporation of the filtrate produced pale-brown crystals that were collected by filtration and air-dried (0.112 g, 60%). $C_{30}H_{44}Cl_2PbN_6O_{13}$ (974.81): calcd. C 36.96, H 4.55, N 8.62; found C 36.83, H 4.65, N 8.72. Λ_M (acetonitrile): 304 cm^{2}Ω^{-1}mol^{-1} (2:1 electrolyte). MS (FAB) = *m/z* (%BPI): 829 (50) $[Pb(L^3)(ClO_4)]^+$, 729 (100) $[Pb(L^3–H)]^+$. IR (KBr): $\tilde{\nu}$ = 1621 [ν(C=N)], 1535 [ν(C=C)], 1464 [δ(N–H)], 1448 [δ(C–H)$_{ar}$], 1343, 1270 [δ(C–H)$_{crown}$], 1116 [ν(C–O)], 754 [π(C–H)], 1091 [ν$_a$(Cl–O)], 626 [δ$_a$(O–Cl–O)] cm^{-1}.

Crystal Structure Determination

Crystal data and details of data collection and refinement are summarized in Table 3. Three-dimensional X-ray data were collected with a Bruker SMART 1000 CCD diffractometer by the *&πη;-ω* scan method. Reflections were measured from a hemisphere of data collected of frames each covering 0.3° in *ω*. Of the 26720 reflections measured for L^1 and the 33146 measured for compound **5**, all were corrected for Lorentz and polarization effects and for absorption by semiempirical methods[32] on the basis of symmetry-equivalent and repeated reflections. Of the 4825 independent reflections measured for the receptor L^1 and 8645 for compound **5**, 2734 and 7598 reflections, respectively, exceeded the significance level $I > 2\sigma I$. Complex scattering factors were taken from the program SHELX97[33] included in the WinGX program system[34] as implemented on a Pentium® computer. The structure of L^1 was solved by direct methods (SHELX97), whereas the structure of **5** was solved by Patterson methods (DIRDIF99).[35] Both structures were refined by full-matrix least-squares methods on F^2. The hydrogen

Table 3. Crystal data and structure refinement for L^1 and **5**.

	L^1	**5**
Empirical formula	$C_{24}H_{30}N_6O_2$	$C_{30}H_{44}CdCl_2N_6O_{13}$
Formula mass	434.54	880.01
Space group	$P12_1/n1$	$P2_1/c$
Crystal system	monoclinic	monoclinic
a [Å]	15.0205(12)	10.760(2)
b [Å]	10.7111(8)	24.614(5)
c [Å]	15.1438(12)	13.688(3)
β [°]	115.412(2)	97.166(4)
V [Å^3]	2200.7(3)	3596.9(13)
Z	4	4
T [K]	100.0(2)	293(2)
λ [Å] (Mo-K_α)	0.71073	0.71073
$D_{calcd.}$ [g cm^{-3}]	1.312	1.625
μ [mm^{-1}]	0.087	0.828
R_{int}	0.1263	0.0265
Reflections measured	26720	33146
Reflections observed	4825	8645
R_1[a]	0.0583	0.0392
wR_2 (all data)[b]	0.1252	0.0992

[a] $R_1 = \Sigma||F_0| - |F_c||/\Sigma|F_0|$. [b] $wR_2 = \{\Sigma[w(||F_0|^2-|F_c|^2)^2]/\Sigma[w(F_0^4)]\}^{1/2}$.

atoms were included in calculated positions and refined by using a riding mode, except for the hydrogen atoms H2 and H6 of L^1, which were freely refined. Refinement converged with allowance for thermal anisotropy of all non-hydrogen atoms.

CCDC 623182 and 623183 contain the supplementary crystallographic data for the structures included in this paper. These data can be obtained free of charge from The Cambridge Crystallographic Data Centre via http://www.ccdc.cam.ac.uk/datarequest/cif.

Computational Methods: The $[M(L^n)]^{2+}$ (M = Cd or Pb, n = 2 or 3) systems were fully optimized in vacuo by using the B3LYP density functional model[36,37] and the Gaussian 03 package (Revision C.01).[38] In these calculations, we used the 6-31G(d) basis set for ligand atoms, while for Cd and Pb the LanL2DZ valence and effective core potential functions were used.[39,40] The stationary points found on the potential energy surfaces as a result of the geometry optimizations have been tested by frequency analysis to represent energy minima rather than saddle points. The relative free energies of the two isomers of $[Pb(L^3)]^{2+}$ were calculated in vacuo at the same computational level, and they include nonpotential energy contributions (that is, zero-point energy and thermal terms) obtained by frequency analysis. Relative free energies of the two isomers of $[Pb(L^3)]^{2+}$ were also calculated in acetonitrile solution (COSMO-RS model).[41] Final free energies include both electrostatic and nonelectrostatic contributions.

Supporting Information (see footnote on the first page of this article): Figures S1 and S2 showing the B3LYP optimized structures of the $[Pb(L^2)]^{2+}$ and $[Pb(L^3)]^{2+}$ systems, Tables S1–S3 reporting ^1H and ^{13}C NMR spectroscopic data of the ligands and Cd^{II} and Pb^{II} complexes and in vacuo optimized Cartesian coordinates [Å] for the $[M(L^2)]^{2+}$ and $[M(L^3)]^{2+}$ systems (M = Cd or Pb).

Acknowledgments

The authors thank Xunta de Galicia (PGIDIT03TAM10301PR and PGIDIT06TAM10301PR) for generous financial support. The authors are indebted to Centro de Supercomputación of Galicia (CESGA) for providing the computer facilities.

[1] See, for instance: a) R. D. Hancock, A. E. Martell, *Chem. Rev.* **1989**, *89*, 1875–1914; b) R. D. Hancock, *Perspectives in Coordination Chemistry* (Eds.: A. F. Williams, C. Floriani, A. Merbach), Verlag HCA, Basel, **1992**, p. 129; c) R. D. Hancock, A. E. Martell, *Supramol. Chem.* **1996**, *6*, 401–407; d) R. D. Hancock, H. Maumela, A. S. de Sousa, *Coord. Chem. Rev.* **1996**, *148*, 315–347; e) B. P. Hay, R. D. Hancock, *Coord. Chem. Rev.* **2001**, *212*, 61–78.
[2] D. J. Cram, *Science* **1988**, *240*, 760–767.
[3] D. J. Cram, J.-M. Lehn, *J. Am. Chem. Soc.* **1985**, *107*, 3657–3658.
[4] A. E. Martell, R. D. Hancock, R. J. Motekaitis, *Coord. Chem. Rev.* **1994**, *133*, 39–65.
[5] J. M. Harrington, S. B. Jones, P. H. White, R. D. Hancock, *Inorg. Chem.* **2004**, *43*, 4456–4463.
[6] a) U. Hahn, M. Elhabiri, A. Trabolsi, H. Herschbach, E. Leize, A. Van Dorsselaer, A.-M. Albrecht-Gary, J.-F. Nierengarten, *Angew. Chem. Int. Ed.* **2005**, *44*, 5338–5341; b) E. C. Constable, C. E. Housecroft, J. N. Lambert, D. A. Malarek, A. Dan, *Chem. Commun.* **2005**, 3739–3741.
[7] L. Shimoni-Livny, J. P. Glusker, C. P. Bock, *Inorg. Chem.* **1998**, *37*, 1853–1867.
[8] W. J. Geary, *Coord. Chem. Rev.* **1971**, *7*, 81–122.
[9] a) X. X. Zhang, A. V. Boedunov, J. S. Bradshaw, N. K. Dalley, X. Kou, R. M. Izatt, *J. Am. Chem. Soc.* **1995**, *117*, 11507–11511; b) D. Ranganathan, V. Haridas, R. Gilardi, I. L. Karle, *J. Am. Chem. Soc.* **1998**, *120*, 10793–10800.
[10] S. Lahiri, J. L. Thompson, J. S. Moore, *J. Am. Chem. Soc.* **2000**, *122*, 11315–11319.
[11] M. González-Lorenzo, C. Platas-Iglesias, F. Avecilla, C. F. G. C. Geraldes, D. Imbert, J.-C. G. Bünzli, A. de Blas, T. Rodríguez-Blas, *Inorg. Chem.* **2003**, *42*, 6946–6954.
[12] E. Quiroz-Castro, S. Bernes, N. Barba-Behrens, R. Tapia-Benavides, R. Contreras, H. Noth, *Polyhedron* **2000**, *19*, 1479–1484.
[13] J.-M. Grevy, F. Tellez, S. Bernes, H. Noth, R. Contreras, N. Barba-Behrens, *Inorg. Chim. Acta* **2002**, *339*, 532–542.
[14] D. Esteban, D. Bañobre, A. de Blas, T. Rodríguez-Blas, R. Bastida, A. Macías, A. Rodríguez, D. E. Fenton, H. Adams, J. Mahía, *Eur. J. Inorg. Chem.* **2000**, 1445–1456.
[15] a) H. Zhang, X. Wang, H. Zhu, W. Xiao, B. K. Teo, *J. Am. Chem. Soc.* **1997**, *119*, 5463–5464; b) P. C. Junk, M. K. Smith, J. W. Steed, *Polyhedron* **2001**, *20*, 2979–2988.
[16] A. H. Bond, R. D. Rogers, *J. Chem. Crystallogr.* **1998**, *28*, 521–527.
[17] N. Kaltsoyannis, *J. Chem. Soc., Dalton Trans.* **1997**, 1–11.
[18] a) C. Piguet, J.-C. G. Bünzli, G. Bernardinelli, C. G. Bochet, P. Froidevaux, *J. Chem. Soc., Dalton Trans.* **1995**, 83–97; b) M. Elhabiri, R. Scopelliti, J.-C. G. Bünzli, C. Piguet, *J. Am. Chem. Soc.* **1999**, *121*, 10747–10762.
[19] a) R. K. Harris, *Nuclear Magnetic Resonance Spectroscopy: A Physicochemnical View*, Pitman, London, **1983**; b) D. Esteban-Gómez, C. Platas-Iglesias, T. Enríquez-Pérez, F. Avecilla, A. de Blas, T. Rodríguez-Blas, *Inorg. Chem.* **2006**, *45*, 5407–5416.
[20] D. C. Bebout, S. W. Stokes, R. J. Butcher, *Inorg. Chem.* **1999**, *38*, 1126–1133.
[21] E. S. Claudio, M. A. ter Horst, C. E. Forde, C. L. Stern, M. K. Zart, H. A. Godwin, *Inorg. Chem.* **2000**, *39*, 1391–1397.
[22] M. González-Lorenzo, C. Platas-Iglesias, F. Avecilla, S. Faulkner, S. J. A. Pope, A. de Blas, T. Rodríguez-Blas, *Inorg. Chem.* **2005**, *44*, 4254–4262.
[23] C. Platas-Iglesias, D. Esteban, V. Ojea, F. Avecilla, A. de Blas, T. Rodríguez-Blas, *Inorg. Chem.* **2003**, *42*, 4299–4307.
[24] C. Platas, F. Avecilla, A. de Blas, T. Rodríguez-Blas, R. Bastida, A. Macias, A. Rodriguez, H. Adams, *J. Chem. Soc., Dalton Trans.* **2001**, 1699–1705.
[25] D. Esteban, C. Platas-Iglesias, F. Avecilla, J. Mahía, A. de Blas, T. Rodríguez-Blas, *Inorg. Chem.* **2002**, *41*, 4337–4347.
[26] G. Berden, W. L. Meerts, E. Jalviste, *J. Chem. Phys.* **1995**, *103*, 9596–9606, and references therein.
[27] J. R. Platt, *J. Chem. Phys.* **1951**, *19*, 101–118.
[28] L. Prodi, M. Montalti, N. Zaccheroni, J. S. Bradshaw, R. M. Izatt, P. B. Savage, *Tetrahedron Lett.* **2001**, *42*, 2941–2944.
[29] N. Su, J. S. Bradshaw, X. X. Zhang, P. B. Savage, K. E. Krakowiak, R. M. Izatt, *J. Heterocycl. Chem.* **1999**, *36*, 771–775.
[30] W. C. Wolsey, *J. Chem. Educ.* **1973**, *50*, A335–A337.
[31] P. Gans, A. Sabatini, A. Vacca, *Talanta* **1996**, *43*, 1739–1753.
[32] *SADABS Area-Detector Absorption Correction*, Siemens Industrial Automation, Inc., Madison, WI, **1996**.
[33] G. M. Sheldrick, *SHELX97* [Includes *SHELXS97*, *SHELXL97*, *CIFTAB*] - Programs for Crystal Structure Analysis (Release 97–2), Institut für Anorganische Chemie der Universität, Tammanstrasse 4, D-3400 Göttingen, Germany, **1998**.
[34] *WinGX*, MS-Windows system of programs for solving, refining and analyzing single-crystal X-ray diffraction data for small molecules, L. J. Farrugia, *J. Appl. Crystallogr.* **1999**, *32*, 837–838.
[35] P. T. Beurskens, G. Beurskens, R. de Gelder, S. Garcia-Granda, R. O. Gould, R. Israel, J. M. M. Smits, *DIRDIF99 Program System*, Crystallography Laboratory, University of Nijmegen, The Netherlands, **1999**.
[36] A. D. Becke, *J. Chem. Phys.* **1993**, *98*, 5648–5652.
[37] C. Lee, W. Yang, R. G. Parr, *Phys. Rev. B* **1988**, *37*, 785–789.
[38] M. J. Frisch, G. W. Trucks, H. B. Schlegel, G. E. Scuseria, M. A. Robb, J. R. Cheeseman, J. A. Montgomery Jr, T. Vreven,

K. N. Kudin, J. C. Burant, J. M. Millam, S. S. Iyengar, J. Tomasi, V. Barone, B. Mennucci, M. Cossi, G. Scalmani, N. Rega, G. A. Petersson, H. Nakatsuji, M. Hada, M. Ehara, K. Toyota, R. Fukuda, J. Hasegawa, M. Ishida, T. Nakajima, Y. Honda, O. Kitao, H. Nakai, M. Klene, X. Li, J. E. Knox, H. P. Hratchian, J. B. Cross, C. Adamo, J. Jaramillo, R. Gomperts, R. E. Stratmann, O. Yazyev, A. J. Austin, R. Cammi, C. Pomelli, J. W. Ochterski, P. Y. Ayala, K. Morokuma, G. A. Voth, P. Salvador, J. J. Dannenberg, V. G. Zakrzewski, S. Dapprich, A. D. Daniels, M. C. Strain, O. Farkas, D. K. Malick, A. D. Rabuck, K. Raghavachari, J. B. Foresman, J. V. Ortiz, Q. Cui, A. G. Baboul, S. Clifford, J. Cioslowski, B. B. Stefanov, G. Liu, A. Liashenko, P. Piskorz, I. Komaromi, R. L. Martin, D. J. Fox, T. Keith, M. A. Al-Laham, C. Y. Peng, A. Nanayakkara, M. Challacombe, P. M. W. Gill, B. Johnson, W. Chen, M. W. Wong, C. Gonzalez, J. A. Pople, *Gaussian 03*, Gaussian Inc., Wallingford CT, **2004**.

[39] P. J. Hay, W. R. Wadt, *J. Chem. Phys.* **1985**, *82*, 270–283.

[40] A description of the basis sets and theory level used in this work can be found in the following: J. B. Foresman, A. E. Frisch, *Exploring Chemistry with Electronic Structure Methods*, 2nd ed., Gaussian Inc., Pittsburgh, PA, **1996**, ch. 5.

[41] F. Eckert, A. Klamt, *AlChE J.* **2002**, *48*, 369–385.

Received: December 20, 2006
Published Online: April 4, 2007

